RSC Advances

PAPER

View Article Online
View Journal | View Issue

Cite this: *RSC Adv.*, 2023, **13**, 26960

Using polyacrylamide hydrogel to adsorb chloride ions in cement-based materials

Chao Wu,[a] Bo Jin,[a] Zhenghui Li,[a] Yuexin Xu,[a] Yutao Ma,[a] Meng Cao,[b] Hui Li,[b] Changmiao Huang,[b] Wanyu Chen [b] and Hao Wu *[a]

Received 20th June 2023
Accepted 30th August 2023

DOI: 10.1039/d3ra04154a

rsc.li/rsc-advances

Concrete material is an important engineering material for modern marine engineering construction, but the presence of chloride ions in sea sand and seawater can cause corrosion of reinforcing steel, which greatly endangers the safety of reinforced concrete structures. Gel is an environmental friendly functional material which has the functions of exchange and adsorption of ions. Therefore, in this paper, polyacrylamide (PAM) gels were prepared for chloride ions adsorption in a reinforced concrete system. The chloride ions adsorption behavior of PAM gel in simulated seawater and cement were investigated and the maximum adsorption capacity of chloride ions in simulated seawater was 32.67 mg g^{-1}. In addition, compared with the cement sample without gel, the chloride ion content in the cement sample containing 1.5 wt% gel was reduced 46.8% at a depth of 0–2.5 mm from the sample's surface. The results showed that PAM gel can effectively adsorb the chloride ion and improve the chloride ion penetration resistance in cement because the three-dimensional network structure of PAM gels allowed chloride ions to enter the inside of the gel. This gel has potential applications in the field of marine construction.

1. Introduction

Gel is a polymer material with a three-dimensional network crosslinked structure.[1,2] The structure of the gel is highly controllable and the functional groups on the polymer chains can be adjusted to make the gel material respond to many environmental stimuli, such as pH, temperature, quantity of electric charge, and magnetic signals.[3–5] And it can also control the porous structure of the gel by adjusting the cross-link density and crosslink strength of the polymer network, so that it has the functions of exchange and adsorption of ions. Therefore, gels are widely used in the fields of biomedical materials, wastewater treatment and energy materials. As an environmental friendly functional material, gel is also being used more and more widely in the field of construction materials. For example, Liu *et al.*[6] designed supramolecular hydrogels as carriers of phosphate for a cement paste self-healing system. When cracks occurred in cement-based materials, the gel responded and released the phosphate. The healing efficiency of this self-healing system can reach 93.2% for resistance to water penetration repair ratio after curing for 28 days.

Concrete material is an important engineering material for modern marine engineering construction such as port terminals, cross-sea bridges, undersea tunnels and island buildings.[7,8] The use of sea sand and seawater instead of traditional river sand and freshwater in the marine engineering concrete materials can be reduced raw material costs and transportation costs.[9] However, the presence of chloride ions in sea sand and seawater can cause corrosion of reinforcing steel, which greatly endangers the stability and safety of reinforced concrete structures.[10] The chloride ions mainly enter the concrete in two ways: external infiltration and internal admixture.[11] The existence of local acidification of chloride ions in concrete can lower the pH of the steel surface to below 4, destroy the passivation film on the surface, form a "corrosion cell" in the local area, accelerate the electrochemical corrosion of the steel. Moreover, the chloride ion will not be consumed, but will act destructively over and over again.[12–14]

At present, in order to reduce the corrosion of reinforcing steel by chloride ions in reinforced concrete system, there are some methods, such as (1) increasing the protective layer of concrete, (2) using concrete surface coating layer, (3) using coated reinforcing steel and corrosion resistant reinforcing steel, (4) mixing with rust inhibitor for reinforcing steel, (5) using cathodic protection for reinforcing steel, (6) maximum control of concrete cracks.[15–17] Thomas M. D. A. *et al.*[18] optimized the chloride curing ability by adding high alumina cement, high strength cement and auxiliary cementitious materials with high Al_2O_3 content to increase Friedel salt production. Z. Shui *et al.*[19] used γ-alumina, γ-alumina hydroxide and nano-alumina colloids to improve the chloride

[a]*General Contracting Co., Ltd of China Construction Third Engineering Bureau Group Co., Ltd, Wuhan, Hubei 430064, China. E-mail: wuhao0489@aliyun.com*
[b]*School of Materials Science and Engineering, Wuhan University of Technology, Wuhan 430070, China*

curing ability of cementitious materials and to form AFm phase more easily. However, the application of gels in the field of chloride ions adsorption in reinforced concrete system is rare.

Gels can be used as adsorptive functional materials. However, studies on the adsorption of chloride ions in concrete by gels are rare and some methods are not suitable for use in buildings because of the high cost of materials. For example, Chen's[20] group studied a kind of double network gel based on chitosan and this gel could adsorb chloride ions in cement. However, chitosan is not suitable for use in real buildings because (1) chitosan is a kind of natural polymer. The amount of chitosan is small in the lab so the consistent of chitosan's solubility can be ensure. But the amount of chitosan is huge if it is used in a whole building so it is difficult to ensure the solubility of chitosan is consistent. (2) Chitosan is too expensive for building materials. Therefore, in this paper, polyacrylamide (PAM) gels which are environmentally compatible[21–23] were prepared for chloride ions adsorption in reinforced concrete system. The chloride ions adsorption behavior of PAM gel in simulated seawater and cement were investigated. The results showed PAM gel could effectively adsorb the chloride ion and improve the chloride ion penetration resistance in cement.

2. Experimental section

2.1. Materials

Acrylamide (Analytical Reagent, 99.0%), tetramethylethylenediamine (99%), calcium chloride anhydrous (99.9%, metals basis), *N*,*N*-methylenebisacrylamide (MBA, 99%) and anhydrous magnesium chloride (99.99%, metals basis) were purchased from Aladdin Technology Co., Ltd (Shanghai, China). *N*,*N*-Dimethylbisacrylamide (DMF, ≥99.5%), ammonium persulfate (≥98.0%), absolute ethanol (≥99.7%), sodium chloride (≥99.8%), sodium sulfate (anhydrous, ≥99.0%), potassium chloride (≥99.8%), sodium bicarbonate (≥99.5%), hydrochloric acid (500 mL, 36.0–38.0%) and sodium hydroxide (flaky, ≥96.0%) were purchased from Sinopharm Chemical Reagent Co., Ltd (Shanghai, China). All the chemicals are analytically pure (AR) grade. 201*7 (360 g), D202 (250 g) and H103 (250 g) were purchased from Zhengzhou Hecheng New Material Technology Co., Ltd (Zhengzhou, China). Standard sand was purchased from Xiamen Aceou Standard Sand Co., Ltd (Xiamen, China).

2.2. Preparation of polyacrylamide gel

The synthetic reaction is shown in Fig. 1. 100 g acrylamide, a certain amount of *N*,*N*-methylenebisacrylamide (MBA) and 0.4 g ammonium persulfate (APS) were added to 800 mL distilled water. After stirring for 5 min, the homogeneously mixed prepolymer solution was poured into the glass container and then increased the temperature to 70 °C. After 3 hours, polyacrylamide gel (PAM) was prepared.

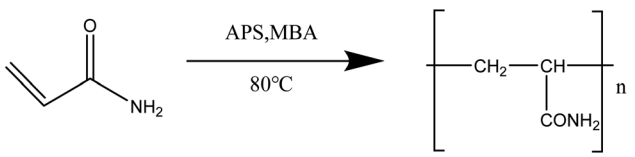

Fig. 1 The synthesis process of PAM gel.

2.3. Pretreatment of resin

H103 is one of the most important polymeric resins with polystyrene skeleton.[24] Pretreatment of H103 resin (purchased from Zhengzhou Hecheng New Material Technology Co., Ltd): 100 g H103 resin was soaked in 95% ethanol solution for 12 hours and then it was washed repeatedly with distilled water. Subsequently, it was soaked with 5 wt% hydrochloric acid solution and rinsed with water until the liquid was neutral. Rinsed with 5 wt% sodium hydroxide solution and washed with water until neutral. Finally the resin was dried in vacuum drying oven.

The matrix of 201*7 is styrene–divinylbenzene, and it's functional group is $-N(CH_3^+)_3$. The matrix of D202 is Styrene–divinylbenzene, and it's functional group is $-N(CH_3^+)_2$-C_2H_4OH.[25] Pretreatment of 201*7 resin and D202 resin (purchased from Xiamen Aceou Standard Sand Co., Ltd): 100 g 201*7 resin or D202 resin was washed with distilled water until the wash solution was colorless. The resin was then soaked in 5% hydrochloric acid solution for 6 h and washed with water to neutral. Soaked the resin in 5 wt% sodium hydroxide solution and washed with water until neutral. Finally the resin was dried in vacuum drying oven.

2.4. Preparation of cement-based materials

Poured a certain quality of Portland cement (PO52.5) into a cement mortar mixer. Added a certain quality of water (cement : sea sand : water (mass ratio) = 2 : 6 : 1) and covered with a blender. After mixing the cement, added a certain quality of sea sand and stirred at high speed for 10 minutes. Added a certain amount of gel and stirred at high speed for 15–20 minutes. The cement mortar mixture was poured into a 20 × 20 × 20 mm cement block mold to fill the mold. Then put the mold on the cement sand vibrating table and shaked for 5 min. After curing at room temperature for 24 hours, the cured mortar sample was obtained. Put the sample in a standard curing room for 28 days.

2.5. Characterization

2.5.1. PAM gel

2.5.1.1. PAM gel infrared spectroscopy test. According to the above preparation method, the reaction solution was dropped onto a glass slide, sealed and placed in a 70 °C oven for 3 h to obtain a PAM gel film. The film was soaked in distilled water for 24 h and changed every 12 h to remove un-reacted monomers and solvents. Then freeze-dried the soaked PAM gel film. The infrared absorption spectra of PAM gel film was determined by Fourier infrared spectrometer (FTIR, Nicolet 6700, Thermo Nicolet Corporation, Massachusetts, USA) with a scanning range of 4000–400 cm^{-1}.

2.5.1.2. PAM gel scanning electron microscopy test. The PAM gel film was freeze-dried for 48 h and then a dry film sample was obtained. The sample was treated with platinum spray and

tested by scanning electron microscopy (SEM, JSM-7500F, JEOL, Tokyo, Japan).

2.5.2. Chloride ions adsorption test

2.5.2.1. Chloride ions adsorption test of PAM gel in simulated seawater. In order to investigate the chloride ions adsorption ability of materials in simulated seaside environments, the simulated seawater was prepared. According to ASTM D1141-98,[26] the composition of simulated seawater are as follows: 12.27 g NaCl, 2.05 g Na_2SO_4, 0.58 g $CaCl_2$, 2.60 g $MgCl_2$, 0.35 g KCl, 0.10 g $NaHCO_3$, 0.05 g KBr, 0.014 g H_3BO_3 and 500 mL deionized water.

Put the PAM gel into the sealed glass bottle containing simulated seawater solution. After shaking for 48 h, took the adsorbed solution from the glass bottle and used Leimagnetic PXSJ-216F ion meter to test the chloride ions content of the solution.

2.5.2.2. Chloride ions adsorption test of resins. Put a certain amount of H103 resin, 201*7 resin and D202 resin in a sealed glass bottle containing simulated seawater, respectively. After soaking for 48 h, took the adsorbed solution from the glass bottle and used Leimagnetic PXSJ-216F ion meter to test the chloride ions content of the solution.

2.5.3. Chloride resistance test of cement-based materials

2.5.3.1. Chloride ion curing test in cement. Cement samples that were cured for 28 days were knocked into powder. Then passed through a 100 mesh sieve to remove the gel from the mortar block. Placed the powder sample in a 100 °C oven and dried to constant weight. The 5 g powder sample was then put in a 250 mL beaker containing 100 mL deionized water. After sealing with plastic wrap, it was placed on a shaker table and continuously shaken for 24 h to completely leach the free chloride ions in the cement powder.

2.5.3.2. Chlorine energy scanning test

EDS test of mortar. Crushed the mortar test block that has been cured for 28 days. Took small pieces with a flat surface. Platinum spraying was applied to cement specimens. It was placed in the SEM sample chamber, and after passing through the selected area of the EM, the elements were scanned with an energy spectrometer with an accelerating voltage of 15 kV.

EDS test of gels. Removed the gel from the simulation experiment and freeze-dry it for 48 h. Dry gels were sprayed with platinum. It was placed in the SEM sample chamber, and after passing through the selected area of the EM, the elements were scanned with an energy spectrometer with an accelerating voltage of 15 kV.

2.5.3.3. Resistance of cementitious materials to chloride ion penetration test. The cement block that had been cured for 24 h was removed from the mold. It was then sealed on all four sides with paraffin, leaving only the two opposite sides. It was soaked in saturated calcium hydroxide solution containing 5% mass fraction sodium chloride at a temperature of 25 °C for 28 days. Then took it out. Wiped dry and placed in an oven for 2 h. The sample was then cut into thin pieces every 2.5 mm from the penetration surface. Its depths were: 0–2.5 mm, 2.5–5 mm, 5–7.5 mm, 7.5–10 mm. These thin pieces were then ground into powder and sieved (100 mesh) to remove the gel. The resulting powder was immersed in quantitative water for 24 h. Tested the chloride content of the immersion solution with an ionometer. The content of chloride ions at different depths from the permeable surface of the cement could be obtained.

3. Results and discussion

3.1. Structure of PAM gel

Fig. 2 showed the FTIR pattern of PAM gel in the range of 4000–400 cm^{-1}. The peak that appears at 3415 cm^{-1} was due to the stretching vibrations of $-NH_2$ and –C–H groups. The peaks at 2936 cm^{-1} and 2860 cm^{-1} were both the stretching vibration peaks of –CH and the peak at 1654 cm^{-1} corresponded to the adsorption band of amide. The peak at 1121 cm^{-1} was related to the stretching vibrations of –C–N in PAM gel and it was the second amide of *N*,*N*-methylenebisacrylamide. This indicated that the formation of crosslinked polyacrylamide.

3.2. Microscopic morphology of PAM gels

Fig. 3 shows the SEM images of PAM gel. As shown in Fig. 3(a), the surface of the PAM gel was rough and had many holes, indicating that the PAM gel had a channel for chloride ions to enter. As shown in Fig. 3(b), the three-dimensional network of the PAM gel were uniform and loose, and the diameters of these pores were about 10 μm. The three-dimensional network

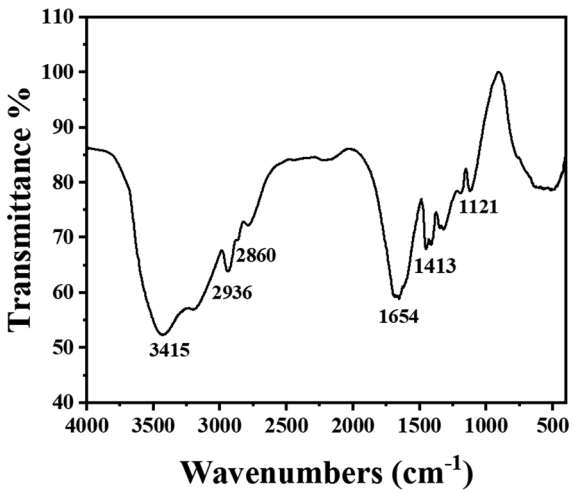

Fig. 2 Infrared spectrum of PAM gel.

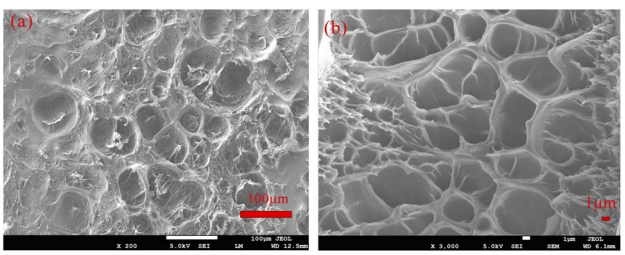

Fig. 3 SEM images of PAM gels at different magnifications. (a) 200 magnifications, (b) 3000 magnifications.

structure of PAM gels could allow chloride ions to enter the inside of the gel.[27–30]

3.3. Chloride ions adsorption of PAM gel in simulated seawater

Fig. 4(a) shows chloride ions adsorption of PAM gels with different crosslinker contents in simulates seawater. When the crosslinker content was 1%, the chloride ions adsorption of PAM gel in simulated seawater was 32.67 mg g^{-1}. With the increase of crosslinker content, the chloride ions adsorption of PAM gels gradually decreased. When the crosslinker content was 9%, the chloride ions adsorption was only 13.63 mg g^{-1}, which was 58.3% lower than the adsorption capacity at 1% crosslinker content. This might be due to the increasing crosslinking density of the polyacrylamide network. When the crosslinker content increased, the three-dimensional network of the PAM gel became more compact and the pore size became smaller, so the chloride ions adsorption of PAM gel was reduced. In addition, when the content of crosslinkers was lower, the active groups on polyacrylamide could form hydrogen bonds with chloride ions. However, with the increasing of the content of crosslinkers, these active groups might be not form hydrogen bonds with chloride ions because they could enter in the crosslinking reaction and the adsorption site was reduced. Thus, the chloride ions adsorption of PAM gel was reduced.

In order to study the effect of monomer content on the chloride ions adsorption of PAM gel, polyacrylamide gels with different acrylamide monomer contents (50 g L^{-1}, 75 g L^{-1}, 100 g L^{-1} and 125 g L^{-1}) were synthesized when the crosslinker content was 1% of the monomer mass. Fig. 4(b) showed the chloride ions adsorption of PAM gels with different acrylamide monomer contents in simulated seawater. When the monomer content was 50 g L^{-1}, the chloride ions adsorption capacity of PAM gel in simulated seawater was 18.96 mg g^{-1}. With the increase of the content of the monomer, the adsorption capacity of PAM to chloride ions gradually increased. When the monomer content was 125 g L^{-1}, the adsorption capacity is 32.67 mg g^{-1}. This was a 72.3% increase in adsorption capacity with a monomer content of 50 g L^{-1}. As the content of the monomer increased, the number of active groups in the PAM chain that could form hydrogen bonds with chloride ions also increased, so the adsorption capacity increased. In addition, when the monomer content was less, the crosslinking density of PAM gel network was smaller and the pore size of three-dimensional network structure was larger.[31,32] The chloride ions captured by the gel through adsorption in simulated seawater were prone to desorption. By comparing the adsorption rate curve in Fig. 4(a) and (b), it could be seen that the change of monomer content had less effect on the chlorine ions adsorption of PAM gel than the change of crosslinker content.[33–39]

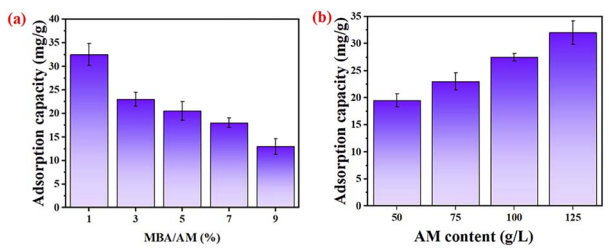

Fig. 4 (a) Chloride ions adsorption of PAM gels with different crosslinker contents in simulate seawater. (b) Chloride ions adsorption of PAM gels with different monomer contents in simulate seawater.

3.4. Adsorption of commercially available resins in simulated seawater

This paper aims at find a new material which can adsorb chlorine ions in cement-based materials. Therefore, it is necessary to study the chlorine ions adsorption capacity. To compare the chloride ions adsorption capacity of PAM gels with commercially available resins, three common commercially available ion exchange resins were selected: macroporous H103 strong alkaline anionic resin, gel type 201*7 strong alkaline anion exchange resin and macroporous D202 strong alkaline anionic resin.

According to Fig. 5, PAM gel had a stronger chloride ions adsorption capacity than H103, 201*7 and D202 resin in simulated seawater. To compare the three kinds of resin, the order of adsorption capacity from high to low was 201*7, D202 and H103 resin. For example, when the concentration is 30 g L^{-1}, the adsorption rate of PAM was 16.03%, and the adsorption rate of the mass of H103 is 8.71%. In addition, with the increase of the mass of PAM gel, 201*7, D202 and H103 resin, the chloride ions adsorption capacities in simulated seawater obviously increased. For example, when the concentration increased from 6 g L^{-1} to 30 g L^{-1}, the adsorption rate of the mass of D202 increased to 2.21 times, while the adsorption rate of the mass of 201 increased to 2.25 times. This is because the number of resin particles increases, the chance of the active site coming into contact with chloride ions increases, and the chloride ions adsorption capacities increases. The ion exchange process occurs by diffusion to the active site through the spacing between its crosslinked points. As shown in Fig. 3, the pores diameters of PAM gel three-dimensional network were

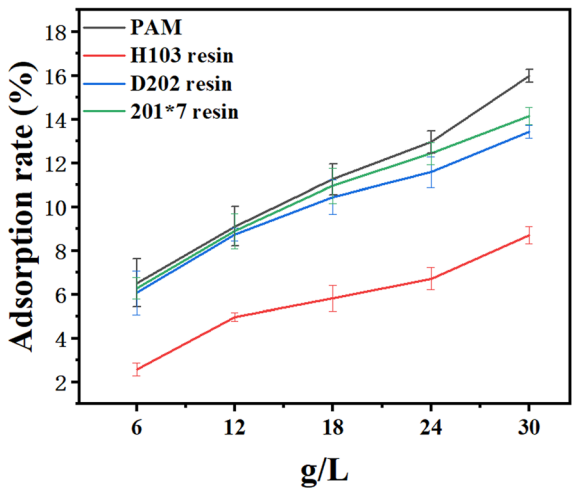

Fig. 5 Adsorption rate of PAM (MBA/PAM is 1%), H103 resin, 201*7 resin and D202 resin in simulated seawater.

about 10 μm. The matrix of gel-type anion exchange resin 201*7 is also microporous and its pore diameter is between 0.5 and 5 nm. The diameter of inorganic ions is about 0.3–0.7 nm.[40–47] Therefore, the chloride ions adsorption capacity of gel-type 201*7 resin is higher than macroporous ion exchange resins H103 and D202. For example, when the concentration was 6 g L^{-1}, the adsorption rate of PAM was 6.525%, and the adsorption rate of the mass of H103 was 2.5875%. In addition, with the increase of the mass of PAM gel, 201*7, D202 and H103 resin, the chloride ions adsorption capacities in simulated seawater obviously increased. For example, when the concentration increased from 6 g L^{-1} to 30 g L^{-1}, the adsorption rate of the mass of D202 increased to 2.2 times, while the adsorption rate of the mass of 201 increased to 2.25 times.

3.5. Adsorption in cement

In order to study the adsorption capacity of PAM on chloride ions in marine architecture, PAM gel was mixed in the cement with sea sand. Fig. 6(a) showed the content of free chloride ion of the cement curing 28 days with gel (1 wt% and 1.5 wt%) and without gel respectively. As shown in Fig. 6(a), the content of free chloride ion of the cement with gel was obviously less than the content of free chloride ion of the cement without gel and the content of free chloride ion decreased when the gel weight was increasing. Compared to the content of free chloride ion of the cement without gel, the contents of free chloride ion of the cement with 1 wt% and 1.5 wt% had decreased by 21.7% and 30.9%, respectively. Fig. 6(b) showed EDS spectra of Cl elements of PAM gel after the gel was mixed in cement for 28 days. PAM gel was polyacrylamide gel and it did not contain chlorine element before it was mixed in cement. However, it could be seen that the relative strength distribution of Cl element in PAM gel which was mixed in cement for 28 days was strong so PAM gel could effectively adsorb chloride ions in cement with sea sand. Fig. 6(c) and (d) showed EDS spectra of Cl element of cement with 1.5 wt% gel and without gel respectively. These figures indicated that PAM gel adsorbed a lot of chloride ions in cement. As mentioned above, the surface of the PAM gel is rough and has many pores so the PAM gel had a channel for chloride ions to enter and could effectively adsorb the chloride ion in cement.[48–52]

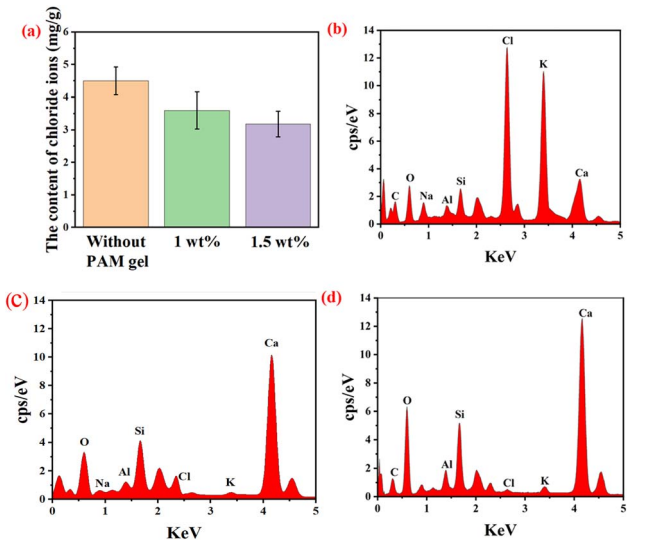

Fig. 6 (a) Content of free chloride ion of the cement curing 28 days with gel (1 wt% and 1.5 wt%) and without gel. (b) EDS spectra of Cl elements of PAM gel after the gel was mixed in cement for 28 days. (c) EDS spectra of Cl element of cement with 1.5 wt% gel. (d) EDS spectra of Cl element of cement without gel.

3.6 Chloride penetration resistance in cement

In order to further study the ability of PAMC gel to adsorb chloride ions in cement, the cement with PAM gels was cured in NaCl solution for 28 days, respectively. The free chloride ion mass fraction at different depths from the surface of cement was measured and showed in Fig. 7. According to Fig. 7, when the depth increased, the content of free chloride ions gradually decreased because chloride ions entered the cement mainly through osmosis. The chloride ion content in the cement with 1.5 wt% gel were 14.3 mg g^{-1} and 2.5 mg g^{-1} at the depth of 0–2.5 mm and 7.5–10 mm, respectively. And the chloride ion content in the cement with 1 wt% gel were 18.2 mg g^{-1} and 3.3 mg g^{-1} at the depth of 0–2.5 mm and 7.5–10 mm, respectively. The free chloride ion content at each depth of the cement without PAM gel group was higher than that of the cement with 1 wt% and 1.5 wt% PAM gel groups. The cement samples containing 1.5 wt% gel had the lowest chloride content at each depth. Compared with the cement sample without gel, the chloride ion content in the cement sample containing 1 wt% gel and 1.5 wt% gel were reduced 31.3% and 46.8% at a depth of 0–2.5 mm, respectively. This showed that when the PAM gel content is higher, it can better prevent the penetration process of chloride ions in cement and improve the resistance of cementitious materials to the chloride ion penetration. This result is consistent with the gel adsorption results in simulated sea water since the amide and hydroxyl groups in PAM gel could

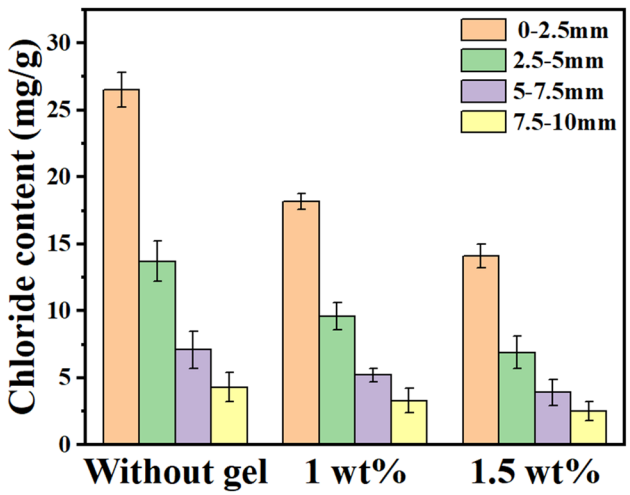

Fig. 7 Chloride ion content of the cement matrix at different depths from the penetration surface after 28 days of maintenance.

form hydrogen bonds with chloride ions to provide adsorption sites.[53–58]

4. Conclusions

In order to reduce the damage of chloride ions to marine structures, PAM gel was prepared for chloride ions adsorption in reinforced concrete system. The chloride ions in simulated seawater were adsorbed by PAM gel and the chloride ions adsorption capacity of PAM gel was stronger than H103, 201*7 and D202 resin in simulated sea-water. In addition, PAM gel could effectively adsorb the chloride ion, such as when the monomer AM content was 125 g L^{-1}, the adsorption capacity was 32.67 mg g^{-1}. The free chloride ion content at each depth of the cement without PAM gel group was higher than that of the cement with 1 wt% and 1.5 wt% PAM gel groups, indicating that PAM gels could effectively prevent the penetration of free chloride ions and improve the chloride ion penetration resistance in cement.

Author contributions

H. W. and W. C. directed the research. C. W., B. J. and Z. L. contributed to the initial idea and experimental design. Y. X., Y. M. and M. C. synthesized the materials and conducted the characterization experiments. C. W., H. L. and C. H. wrote the first manuscript and all authors discussed and revised the manuscript.

Conflicts of interest

There are no conflicts to declare.

Notes and references

1 C. Zhang, Y. Dai, Y. Wu, G. Lu, Z. Cao, J. Cheng, K. Wang, H. Yang, Y. Xia, X. Wen, W. Ma, C. Liu and Z. Wang, *Carbohydr. Polym.*, 2020, **234**, 115882.
2 M. M. Viana, S. Z. S. Do Amparo, M. C. F. S. Lima, R. C. F. G. Lopes, C. K. B. Vasconcelos, V. Caliman and G. G. Silva, *J. Environ. Chem. Eng.*, 2020, **8**, 104415.
3 G. R. Quezada, R. E. Rozas and P. G. Toledo, *Miner. Eng.*, 2021, **162**, 106741.
4 W. Zou, L. Gong, J. Huang, M. Pan, Z. Lu, C. Sun and H. Zeng, *Miner. Eng.*, 2019, **141**, 105841.
5 E. Binaeian, S. Babaee Zadvarzi and D. Yuan, *Int. J. Biol. Macromol.*, 2020, **162**, 150–162.
6 X. Liu, Q. Li, B. Li and W. Chen, *Cem. Concr. Res.*, 2021, **144**, 106427.
7 J. Liu, C. Liao, H. Jin, Z. Jiang and H. Zhou, *Constr. Build. Mater.*, 2021, **302**, 124160.
8 D. V. Ribeiro, S. A. Pinto, N. S. Amorim Júnior, J. S. Andrade Neto, I. H. L. Santos, S. L. Marques and M. J. S. França, *Cem. Concr. Compos.*, 2021, **122**, 104114.
9 S. Han, J. Zhong, W. Ding and J. Ou, *Constr. Build. Mater.*, 2021, **295**, 123703.
10 D. Pan, S. A. Yaseen, K. Chen, D. Niu, C. K. Ying Leung and Z. Li, *Journal of Building Engineering*, 2021, **42**, 103006.
11 J. Liu, X. Fan, J. Liu, H. Jin, J. Zhu and W. Liu, *Constr. Build. Mater.*, 2021, **307**, 124986.
12 C. Yang, L. Li and J. Li, *Constr. Build. Mater.*, 2020, **263**, 120172.
13 L. Xiao, D. Chen, M. Jiang, L. Xiao and G. Mei, *Constr. Build. Mater.*, 2021, **304**, 124576.
14 A. Kenny and A. Katz, *Constr. Build. Mater.*, 2020, **244**, 118376.
15 S. I. Basha, M. A. Aziz, S. Ahmad, M. M. Al-Zahrani, M. Shameem and M. Maslehuddin, *Constr. Build. Mater.*, 2022, **325**, 126812.
16 Z. Shi, M. R. Geiker, B. Lothenbach, K. De Weerdt, S. F. Garzón, K. Enemark-Rasmussen and J. Skibsted, *Cem. Concr. Compos.*, 2017, **78**, 73–83.
17 F. Bolzoni, A. Brenna and M. Ormellese, *Cem. Concr. Res.*, 2022, **154**, 106719.
18 M. D. A. Thomas, R. D. Hooton, A. Scott and H. Zibara, *Cem. Concr. Res.*, 2012, **42**, 1–7.
19 R. Yang, R. Yu, Z. Shui, X. Gao, X. Xiao, X. Zhang, Y. Wang and Y. He, *J. Cleaner Prod.*, 2019, **240**, 118157.
20 M. Cao, L. Wu, G. Zhang, Y. Yang, W. Chen, Q. Li, P. Tang and W. Chen, *Polymers*, 2022, **14**, 2081.
21 S. Moulay, N. Bensacia, F. Garin, I. Fechete and A. Boos, *Adsorpt. Sci. Technol.*, 2013, **31**, 691–709.
22 M. A. M. Ali, A. M. Alsabagh, M. W. Sabaa, R. A. El-Salamony, R. R. Mohamed and R. E. Morsi, *Iran. Polym. J.*, 2020, **29**, 455–466.
23 H. Ji, X. Song, H. Cheng, L. Luo, J. Huang, C. He, J. Yin, W. Zhao, L. Qiu and C. Zhao, *ACS Appl. Mater. Interfaces*, 2020, **12**, 31079–31089.
24 Y. Shan, Y. Song, Y. Liu, R. Liu, J. Du and P. Zeng, *Environ. Earth Sci.*, 2015, **73**, 4989–4994.
25 W.-L. Wu, Z.-Q. Tan, G.-J. Wu, L. Yuan, W.-L. Zhu, Y.-L. Bao, L.-Y. Pan, Y.-J. Yang and J.-X. Zheng, *Sep. Purif. Technol.*, 2013, **102**, 163–172.
26 ASTM D1141-1998 Standard Practice for the Preparation of Substitute Ocean Water, ASTM International, West Conshohocken, Pennsylvania, 2021.
27 T. Wang, W. Zhao, Y. Wu, X. Wang, A. B. Kayitmazer, A. Ahmad, N. Ramzan, Y. Si, J. Wang and Y. Xu, *ACS Appl. Polym. Mater.*, 2023, **5**, 1169–1179.
28 S. Nagashima, N. Akamatsu, X. Cheng, S. Matsubara, S. Ida, H. Tanaka, M. Uchida and D. Okumura, *Langmuir*, 2023, **39**, 3942–3950.
29 H. Cai, Z. Chen, S. Guo, D. Ma and J. Wang, *Sol. Energy Mater. Sol. Cells*, 2023, **256**, 112310.
30 J. Mazuryk, K. Klepacka, J. Piechowska, J. Kalecki, L. Derzsi, P. Piotrowski, P. Paszke, D. A. Pawlak, S. Berneschi, W. Kutner and P. S. Sharma, *ACS Appl. Polym. Mater.*, 2023, **5**, 223–235.
31 M. B. Bilgic, K. Kaya, N. Orakdogen and Y. Yagci, *Eur. Polym. J.*, 2022, **167**, 111062.
32 Y. Wang, G. Nian, J. Kim and Z. Suo, *J. Mech. Phys. Solids*, 2023, **170**, 105099.

33 J. Kim, T. Yin and Z. Suo, *J. Mech. Phys. Solids*, 2022, **168**, 105017.
34 A. Rahmatpour, N. Alijani and A. Mirkani, *React. Funct. Polym.*, 2023, **185**, 105537.
35 D. Zhu, M. Miao, X. Du, Y. Peng, Z. Wang, S. Liu and J. Xing, *Eur. Polym. J.*, 2022, **174**, 111327.
36 Y. Bai, Y. Lian, C. Ban, Z. Wang, J. Zhao and H. Zhang, *J. Mol. Liq.*, 2021, **329**, 115578.
37 Q.-F. Li, S. Sun, S. Chu, L. Jin, J.-T. Wang and Z. Wang, *Polymer*, 2021, **236**, 124319.
38 F. Hakiki and F. Arifurrahman, *J. Ind. Eng. Chem.*, 2023, **119**, 532–549.
39 M. A. Corona Rivera, C. A. Cisneros Covarrubias, V. V. A. Fernández Escamilla, E. Mendizábal Mijares and J. E. Pérez López, *Polym. Eng. Sci.*, 2022, **62**, 1797–1810.
40 X. Zhu, W. Li and C. Zhang, *Environ. Res.*, 2020, **180**, 108865.
41 Y. Shan, Y. Song, Y. Liu, R. Liu, J. Du and P. Zeng, *Environ. Earth Sci.*, 2015, **73**, 4989–4994.
42 K. Xiao, F. Xu, L. Jiang, Z. Dan and N. Duan, *Chemosphere*, 2016, **156**, 326–333.
43 W.-L. Wu, Z.-Q. Tan, G.-J. Wu, L. Yuan, W.-L. Zhu, Y.-L. Bao, L.-Y. Pan, Y.-J. Yang and J.-X. Zheng, *Sep. Purif. Technol.*, 2013, **102**, 163–172.
44 M. Parvazinia, S. Garcia and M. Maroto-Valer, *Chem. Eng. J.*, 2018, **331**, 335–342.
45 Z. Zhao, F. Hu, Y. Hu, S. Wang, P. Sun, G. Huo and H. Li, *Int. J. Refract. Hard Met.*, 2010, **28**, 633–637.
46 C. Ma, T. Liu, L. Yang, Y. Zu, F. Yang, C. Zhao, L. Zhang and Z. Zhang, *J. Chromatogr. B*, 2011, **879**, 3444–3451.
47 L.-L. Wei, G.-Z. Wang, J.-Q. Jiang, G. Li, X.-L. Zhang, Q.-L. Zhao and F.-Y. Cui, *Desalin. Water Treat.*, 2015, **56**, 1633–1647.
48 X. Liu, R. Liu, X. Xie, J. Zuo, K. Lyu and S. P. Shah, *Constr. Build. Mater.*, 2023, **364**, 129907.
49 L. Tong, J. Zhao and Z. Cheng, *Constr. Build. Mater.*, 2021, **309**, 125126.
50 R. Gunawan, M. Yang and C. Lau, *Talanta Open*, 2023, **7**, 100189.
51 J. Mao, Y. Liu, J. Xu, Q. Wang and Y. Lou, *Constr. Build. Mater.*, 2023, **362**, 129680.
52 Y. Ma, Y. Ge, R. Wu, H. Huang, G. Chen, Y. Xu, J. Liu, P. Zhang and F. Xiao, *Constr. Build. Mater.*, 2022, **340**, 127765.
53 Y. Yu and L. Lin, *Constr. Build. Mater.*, 2020, **264**, 120620.
54 B. Song, C. Shi, X. Hu, K. Ouyang, Y. Ding and G. Ke, *Constr. Build. Mater.*, 2021, **288**, 123113.
55 L. Caneda-Martínez, M. Frías, C. Medina, M. I. S. de Rojas, N. Rebolledo and J. Sánchez, *Constr. Build. Mater.*, 2018, **190**, 200–210.
56 L. Kang, Y. Shi and X. Luo, *AIP Adv.*, 2021, **11**, 015118.
57 C. Bertin and A. C. M. Bourg, *Environ. Sci. Technol.*, 1994, **28**, 794–798.
58 J. H. She, P. Mechnich, H. Schneider, B. Kanka and M. Schmücker, *J. Mater. Sci. Lett.*, 2000, **19**, 1887–1891.